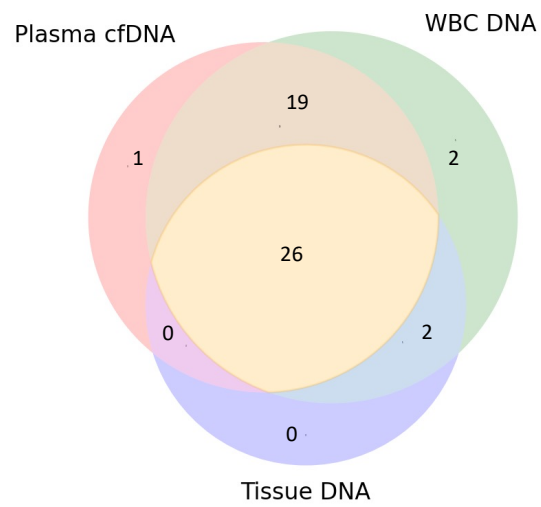


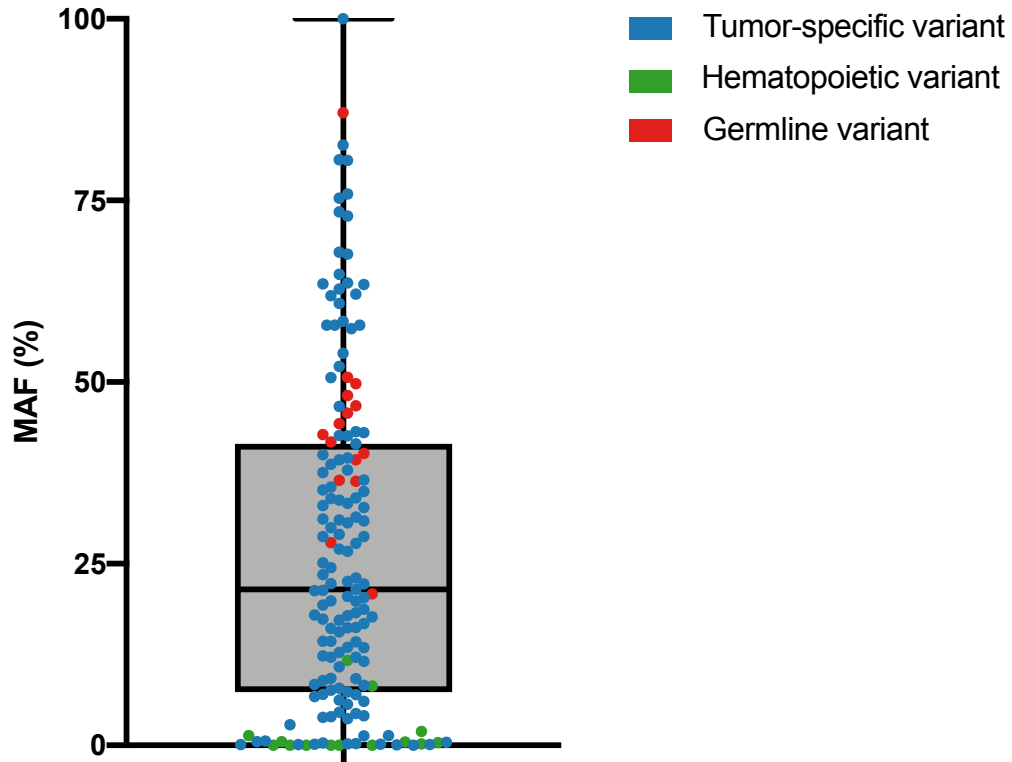
## **Supplementary Figures**

**Metastatic colorectal cancer treatment response evaluation by ultra-deep sequencing of cell-free DNA and matched white blood cells**

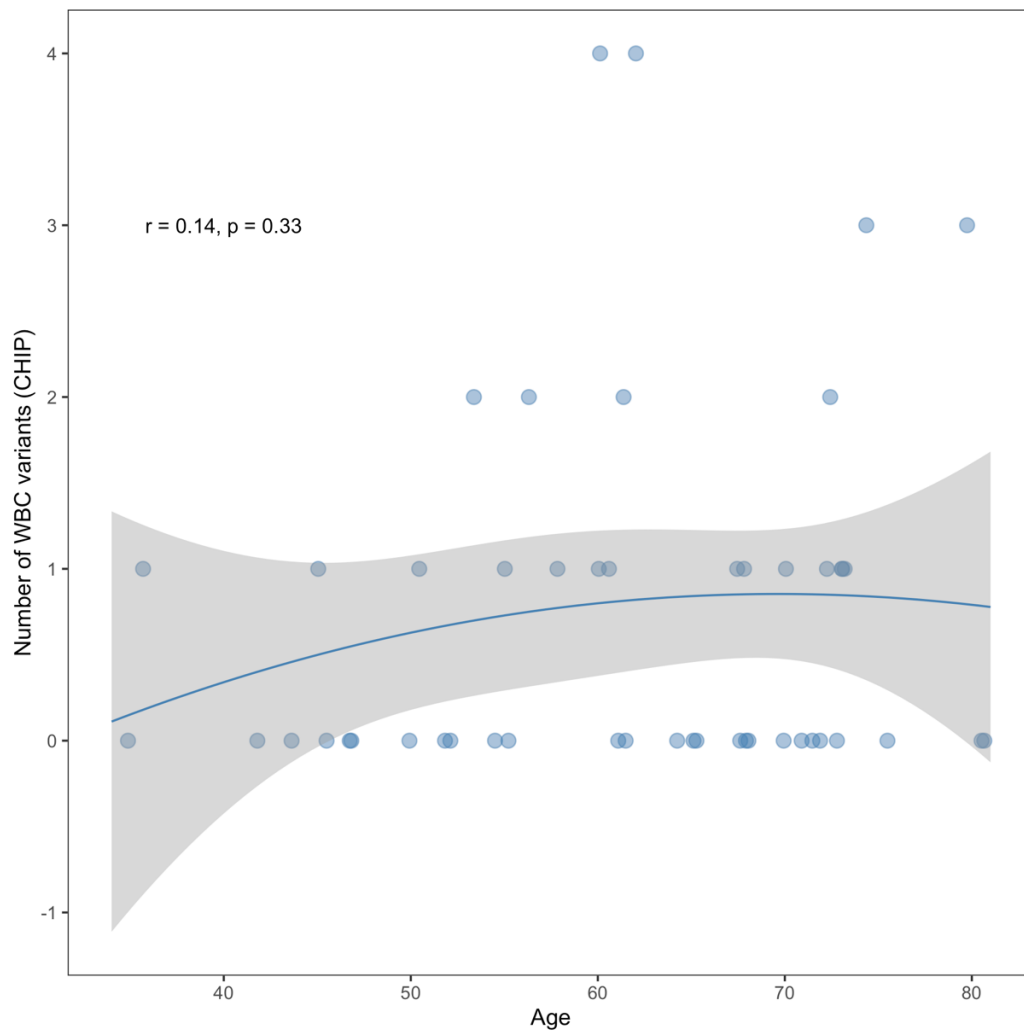
van 't Erve & Medina *et al.*



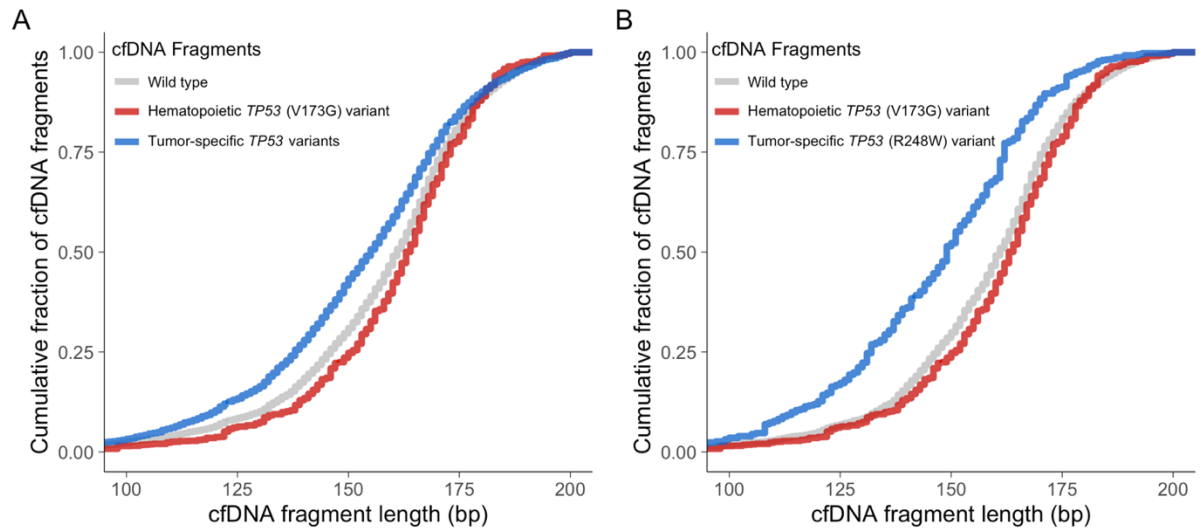
**Supplementary Figure 1.** Venn diagram of patient-matched plasma cell-free DNA, blood-derived WBC genomic DNA, and tumor tissue DNA samples at baseline, *i.e.* before treatment initiation. Abbreviations: cfDNA; cell-free DNA. WBC; white blood cell.



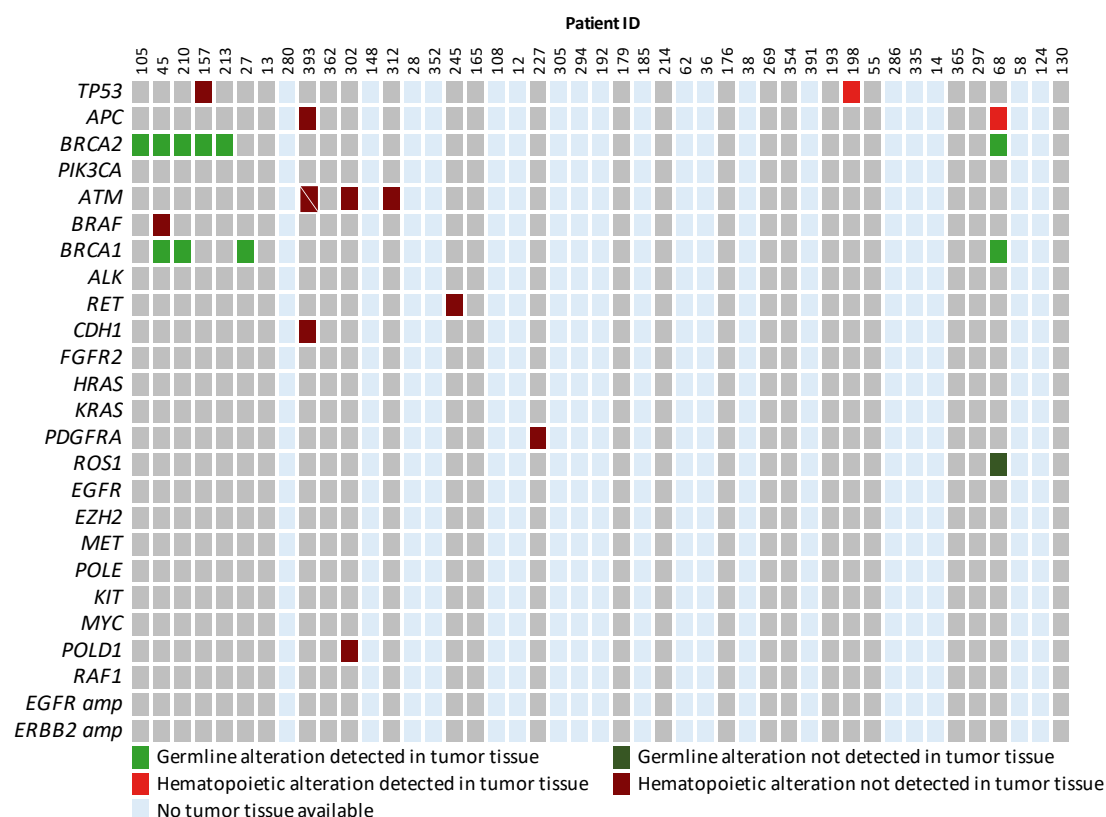
**Supplementary Figure 2.** MAFs of plasma ctDNA tumor-specific variants (blue) and filtered hematopoietic (green) and germline alterations (red) based on WBC genomic DNA, identified in baseline cfDNA samples of 45 patients. Abbreviations: cfDNA; cell-free DNA. MAF; mutant allele frequency. WBC; white blood cell.



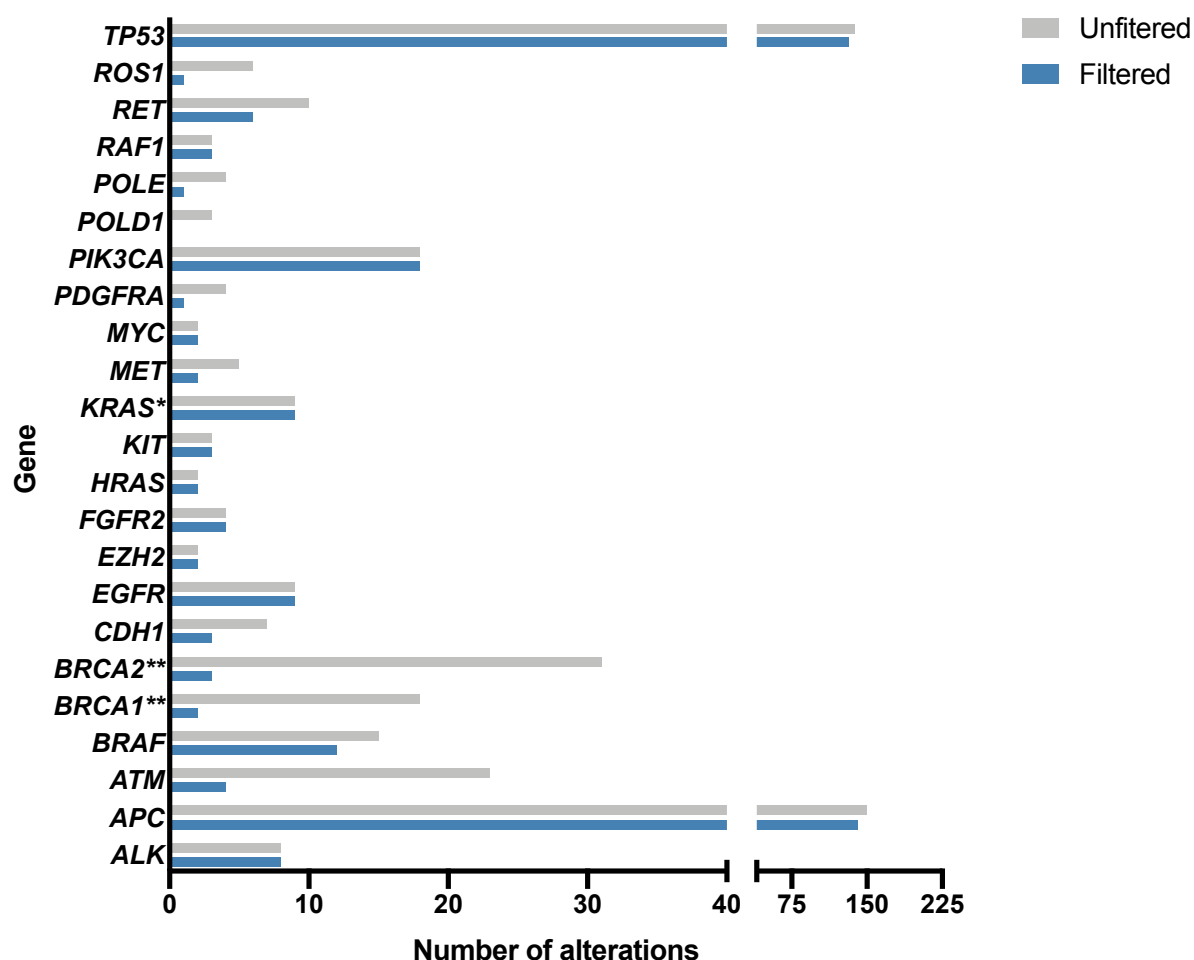
**Supplementary Figure 3.** Association between age (x-axis) and the absolute number of detected WBC variants (y-axis) with Pearson correlation  $r=0.14$  ( $p=0.33$ ). Abbreviation: WBC; white blood cell.



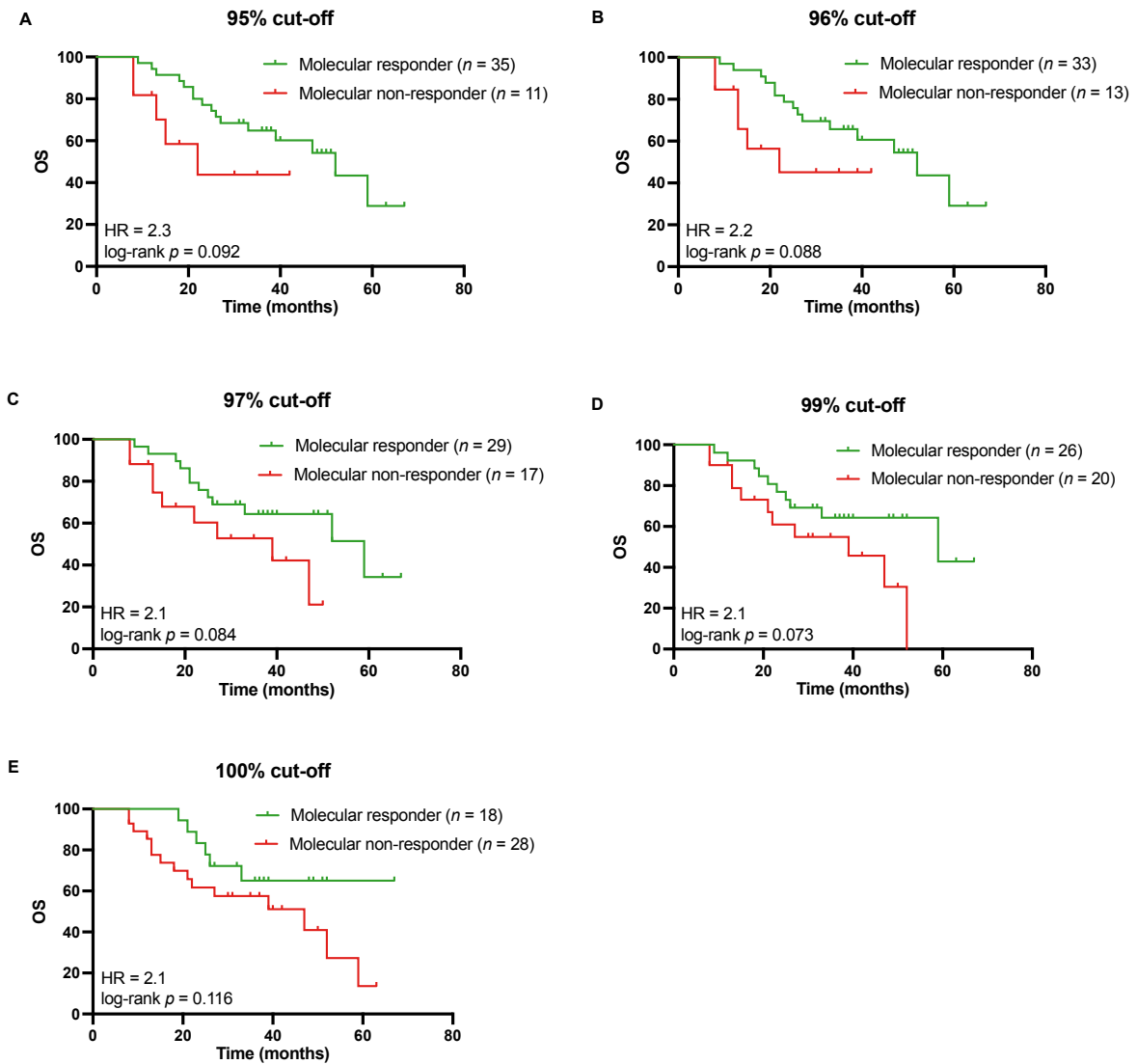
**Supplementary Figure 4.** *TP53* variants detected across multiple patients in tumor-tissue DNA, WBC genomic DNA, and cfDNA. **(A)** Cumulative fraction of cfDNA fragment lengths (bp) for *TP53* (V173G) hematopoietic variant (red) compared to *TP53* wildtype (grey) and tumor-specific variants in multiple patients (blue) (wildtype vs tumor-specific *TP53*, Kolmogorov–Smirnov test,  $p < 0.001$ ; *TP53* (V173G) hematopoietic variant vs tumor-specific *TP53*, Kolmogorov–Smirnov test,  $p < 0.001$ ). **(B)** Patient 198 harbored a *TP53* V173G variant (red) and a *TP53* R248W variant (blue). The *TP53* V173G variant was detected in tumor-tissue, WBCs, and cfDNA, whereas the *TP53* R248W was only detected in the cfDNA and tumor tissue but not within WBCs. Cumulative fragment lengths could distinguish the hematopoietic *TP53* V173G variant from the tumor-specific *TP53* R248W variant (*TP53* V173G hematopoietic variant vs tumor-specific *TP53* R248W, Kolmogorov–Smirnov test,  $p < 0.001$ ). Abbreviations: cfDNA; cell-free DNA. WBC; white blood cell.



**Supplementary Figure 5.** WBC alterations detected in tumor tissue. Sequencing of patient-matched tumor tissue DNA available for 26 out of 45 patients identified nearly all germline alterations (light green), but nearly none of the hematopoietic alterations (dark red) found upon sequencing patient-matched WBC-derived genomic DNA. Interestingly, the TP53 alteration of patient 198 had a tumor tissue MAF of 5% and a plasma cfDNA MAF of 12%, which might be interpreted as a tumor-specific somatic mutation that could be detected as ctDNA in plasma. However, WBC analyses reported a MAF of 14%, implying this TP53 alteration is a hematopoietic variant as also supported by cfDNA fragment length analysis (Supplementary Figure 4B). This example illustrates that tumor tissue-informed ctDNA analysis can result in false positives when WBC alterations are detected in tissue material. Abbreviations: cfDNA; cell-free DNA. MAF; mutant allele frequency. WBC; white blood cell.

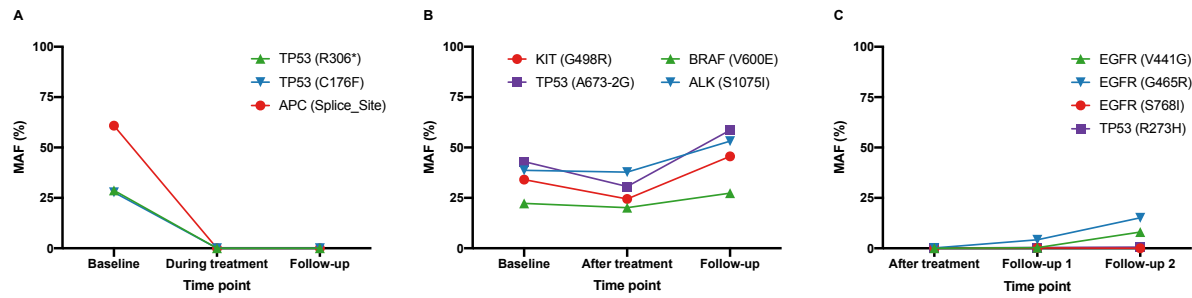


**Supplementary Figure 6.** Number of alterations per gene identified before (gray) and after (blue) filtering of hematopoietic and germline alterations based on WBC genomic DNA. \*Patients included in the CAIRO5 trial were tested in routine diagnostics for *KRAS*, *NRAS*, and *BRAF* tumor tissue mutation status and were initially *RAS/RAF* wildtype at inclusion. However, plasma deep-sequencing revealed baseline *KRAS* alterations. Non-hotspot mutations in combination with the used tumor tissue mutation assays, or tumor heterogeneity, might explain these discordant results, as discussed previously(26). \*\**BRCA* sequence variants were reported at any MAF and not excluded from reporting in the pipeline based on MAF, allowing clinical reviewing of the detected *BRCA* alterations. Abbreviations: MAF; mutant allele frequency. WBC; white blood cell.

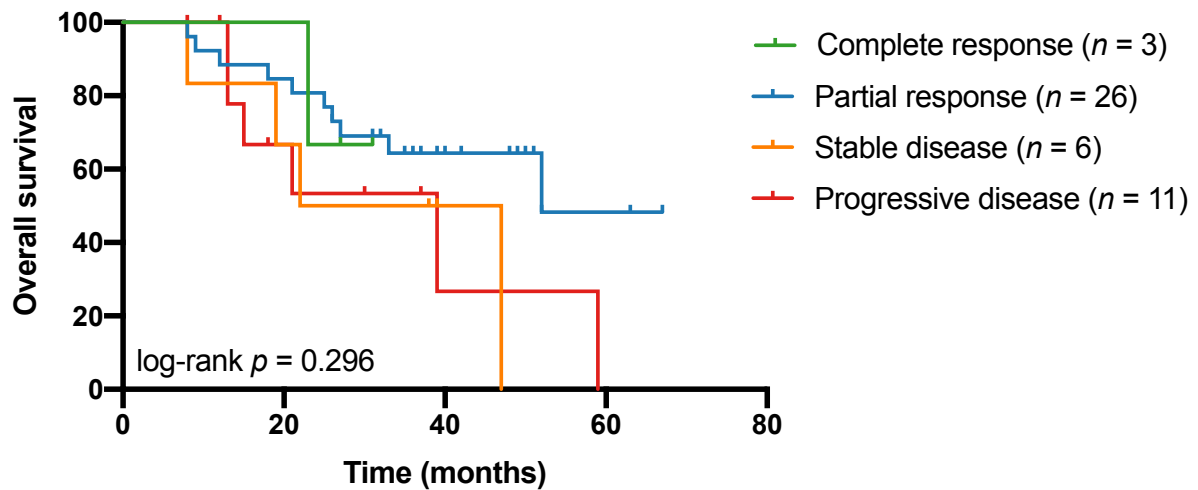


**Supplementary Figure 7.** Different cut-off points for calling a patient a molecular responder based on ctDNA analyses after treatment compared to baseline were evaluated, **(A)** 95%, **(B)** 96%, **(C)** 97%, **(D)** 99%, and **(E)** 100%. The 98% cut-off is depicted in Figure 5A.

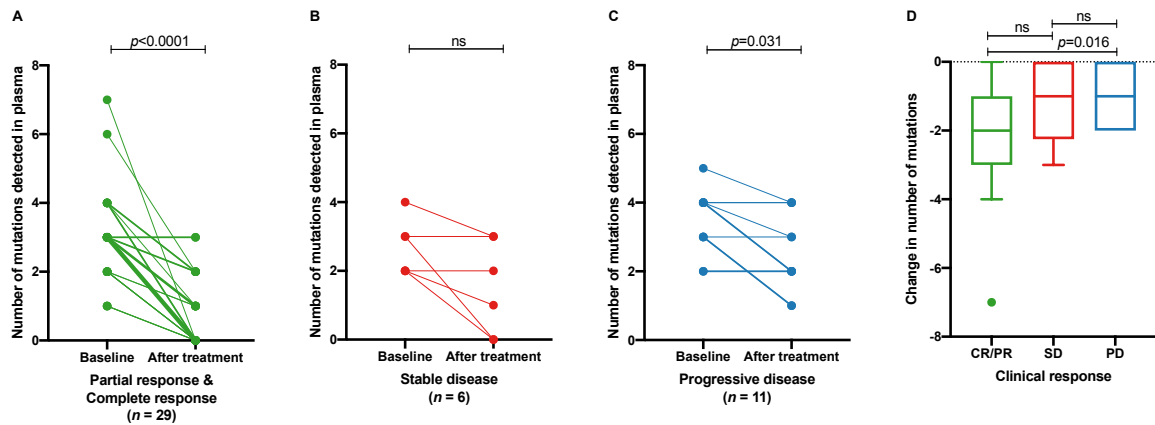




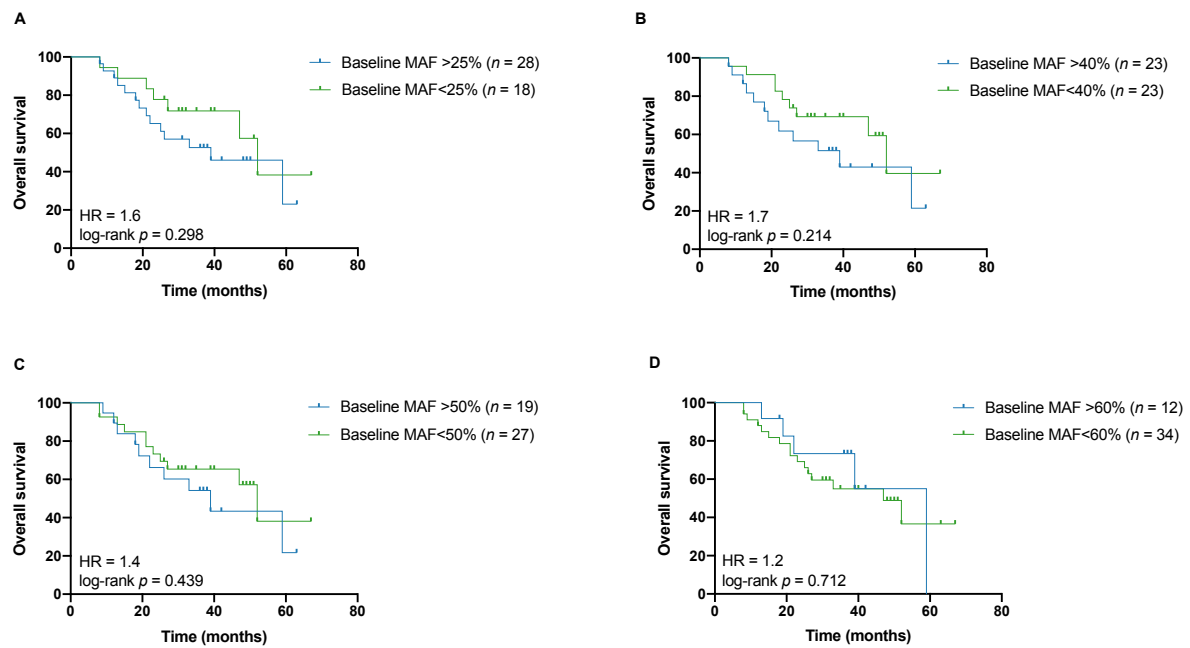
**Supplementary Figure 8.** Molecular responders and non-responders to treatment. Longitudinal plasma ctDNA MAFs of identified somatic mutations of **(A)** a patient classified as a molecular responder by clearance of all ctDNA upon treatment, **(B)** a patient classified as a molecular non-responder to treatment by MAF levels that do not drop below 20% and **(C)** a patient showing acquired resistance with increases in MAFs of EGFR ectodomain mutations. Abbreviation: MAF; mutant allele frequency.



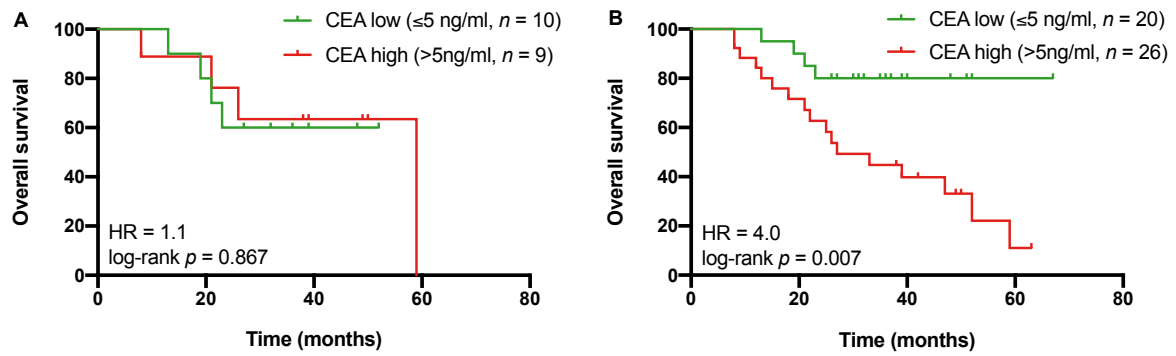
**Supplementary Figure 9.** Overall survival and radiological response evaluation of CT images (log-rank  $p=0.296$ ). The molecular response was defined as ctDNA clearance over 98% upon treatment compared to the initial ctDNA measurement. The radiological response was based on RECIST. Median survival was 39 months for patients with progressive disease, 35 months for patients with stable disease, 52 months for patients with partial response, and undefined for the patients with complete response. Abbreviations: ctDNA; circulating tumor DNA. CT; computed tomography. RECIST; Response Evaluation Criteria in Solid Tumors.



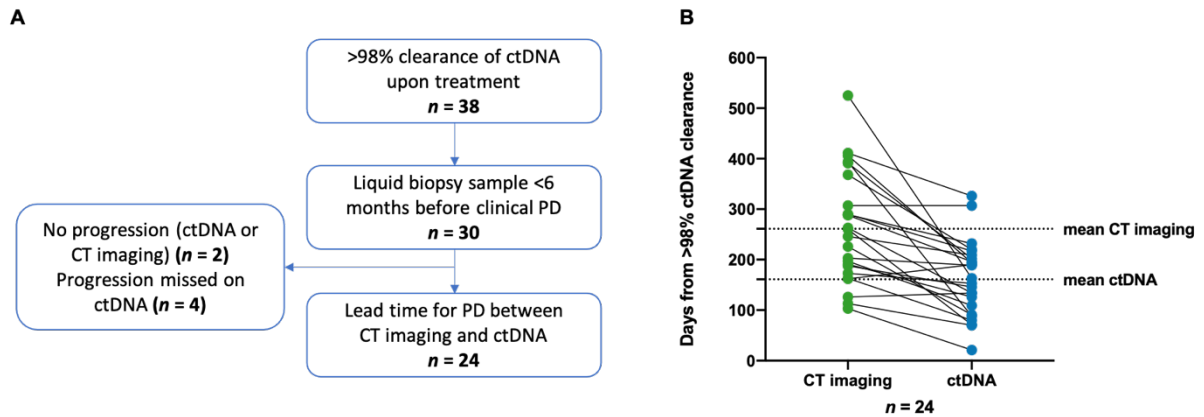
**Supplementary Figure 10.** The number of mutations detected in plasma at baseline and after treatment in patients with a radiological **(A)** partial or complete response ( $p < 0.0001$ ), **(B)** stable disease ( $p = 0.125$ ), or **(C)** progressive disease ( $p = 0.031$ ), compared between Wilcoxon matched-pairs signed-rank tests. **(D)** The change in the number of mutations detected was significant between patients with a partial or complete response (PR/CR) compared to patients with progressive disease (PD) assessed by one-way ANOVA Tukey's multiple comparison testing ( $p = 0.016$ ). Abbreviations: ns; not significant.



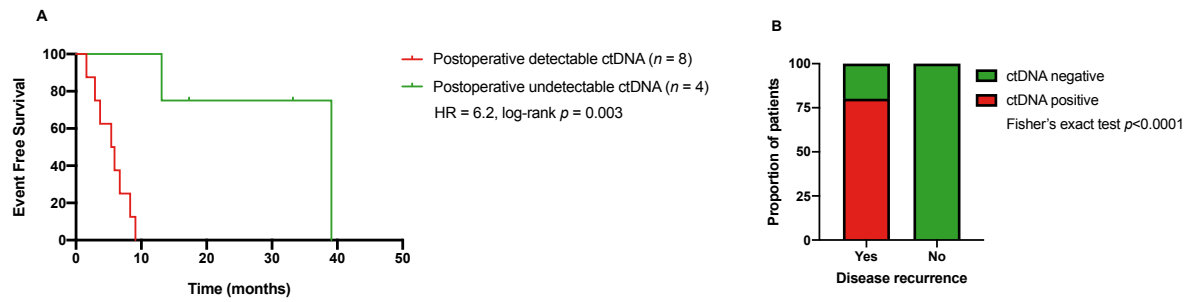
**Supplementary Figure 11.** Absolute baseline ctDNA levels at different cutoffs (based on the median and interquartile range); **(A)** 25%, **(B)** 40%, **(C)** 50%, and **(D)** 60% were not prognostic for overall survival (log-rank  $p=0.298$ ,  $p=0.214$ ,  $p=0.439$ ,  $p=0.712$ , respectively). Abbreviations: MAF; mutant allele frequency. HR; hazard-ratio.



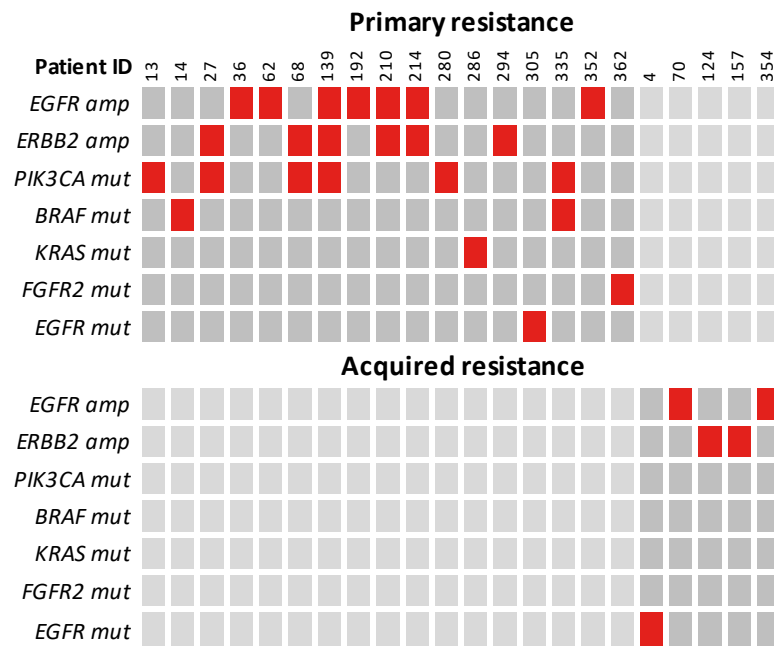
**Supplementary Figure 12.** Response evaluation based on serum CEA. **(A)** Patients were evaluated with a CEA measurement within a range of one month from the ctDNA measurement after treatment. CEA levels after treatment were not prognostic for overall survival. **(B)** Patients with all longitudinal CEA measurements after treatment below 5 ng/ml showed better overall survival than patients with one or more CEA levels above 5 ng/ml (HR=4.0; 95% CI=1.7–9.4; log-rank  $p=0.007$ ). Abbreviations: CEA; carcinoembryonic antigen. HR; hazard-ratio.



**Supplementary Figure 13. (A)** From the 38 patients with a molecular response to treatment, *i.e.* elimination of >98% of ctDNA, lead time till disease recurrence could be evaluated for 30 patients with a blood sample at least six months before clinical disease progression. Disease progression was missed upon ctDNA analyses of four patients, and two patients showed no progression of the disease, leaving 24 patients for lead time analyses. **(B)** A median lead time of ctDNA over CT imaging of 3.2 months was observed (Wilcoxon matched-pairs signed-rank test;  $p < 0.001$ ). Abbreviations: CT; computed tomography. ctDNA; circulating tumor DNA. PD; progression of disease.



**Supplementary Figure 14. (A)** EFS calculated as the time from surgery to disease recurrence or death, whichever came first, for the patients with postoperative ctDNA (HR=6.2; 95% CI=1.7–22.1; log-rank  $p=0.003$ ). **(B)** The association between postoperative disease recurrence and ctDNA outcome (Fisher's exact test  $p<0.0001$ ). Abbreviations: ctDNA; circulating tumor DNA. EFS; event-free survival. HR; hazard-ratio.



**Supplementary Figure 15.** Identified mechanisms of primary resistance (top panel) and acquired resistance (bottom panel) in 22 out of 52 patients (42%) compared by Fisher's exact testing ( $p=0.159$ ). Although patients with mutations in *KRAS* (from the start of the study) and *BRAF* (from patient 156 onwards) in the tumor tissue had been excluded from this arm of the CAIRO5 study, we detected a *KRAS* and *BRAF* hotspot alteration pointing toward tumor heterogeneity.